REVIEW ARTICLE

Ultrasound in decompression research: fundamentals, considerations, and future technologies

David Q. Le, BS [1]; Paul A. Dayton, PhD [1]; Frauke Tillmans, PhD [2]; John J. Freiberger, MD [3]; Richard E. Moon, MD [3]; Petar Denoble, MD [2]; Virginie Papadopoulou, PhD [1]

[1] Joint Department of Biomedical Engineering, The University of North Carolina at Chapel Hill and North Carolina State University, Chapel Hill, North Carolina, U.S.

[2] Divers Alert Network, Durham, North Carolina, U.S.

[3] Center for Hyperbaric Medicine and Environmental Physiology, Duke University, North Carolina, U.S.

CORRESPONDING AUTHOR: Virginie Papadopoulou – *papadopoulou@unc.edu* or *virginiepapadopoulou@gmail.com*

ABSTRACT

It is widely accepted that bubbles are a necessary but insufficient condition for the development of decompression sickness. However, open questions remain regarding the precise formation and behavior of these bubbles after an ambient pressure reduction (decompression), primarily due to the inherent difficulty of directly observing this phenomenon in vivo. In decompression research, information about these bubbles after a decompression is gathered via means of ultrasound acquisitions. The ability to draw conclusions regarding decompression research using ultrasound is highly influenced by the variability of the methodologies and equipment utilized by different research groups. These differences play a significant role in the quality of the data and thus the interpretation of the results. The purpose of this review is to provide a technical overview of the use of ultrasound in decompression research, particularly Doppler and brightness (B)-mode ultrasound. Further, we will discuss the strengths and limitations of these technologies and how new advancements are improving our ability to understand bubble behavior post-decompression. ∎

INTRODUCTION

Context

Decompression sickness (DCS) is a condition that arises when decompression of the human body allows for the formation of gas bubbles that lead to physiological symptoms ranging from skin itching and neurological problems to excruciating pain, coma and even death [1]. The rapid reduction in pressure resulting in DCS is seen in altitude expeditions, space flight and extravehicular activities, hyperbaric tunneling work, and scuba diving [1-3].

The earliest evidence of in vivo decompression bubbles was observed in 1670 by Robert Boyle, when a viper placed in a vacuum chamber was observed to have bubbles forming in its eye [4]. In 1878, Paul Bert found a connection between DCS in caisson workers and bubble formation [5]. This was later replicated in work by Leonard Hill and JJR Macleod in the early 1900s, who also observed bubbles in a frog's web and bat's wing [6].

Specific to scuba diving, divers breathe gas mixtures delivered at ambient pressures throughout the dive. As the diver descends in the water column, the ambient pressure increases, resulting in larger partial pressures for oxygen and inert gases that the diver breathes. Due to the increased pressures the inert gases readily dissolve into tissue until saturation. Once a diver ascends, the pressure gradient reverses and the tissues "offgas." This creates bubbles known as venous gas emboli (VGE) when they enter the bloodstream and can be detected using ultrasonography [1]. The formation and growth of these bubbles is understood to be the cause of DCS symptoms, either by direct interaction with tissues or a cascade of biochemical events [1,7-9]. However, open questions remain regarding the precise formation and behavior of these bubbles after an ambient pressure reduction (decompression), primarily due to the inherent difficulty of directly observing this phenomenon in vivo [10,11].

KEYWORDS: bubbles; decompression sickness; diving research; Doppler; echocardiography; scuba diving; venous gas emboli

Apart from ultrasound, several imaging modalities have been used to study the formation of decompression bubbles. Early studies into decompression in animals utilized microscopy to observe bubbles in animal models following decompression and freeze-drying [12, 13]. Advancements have allowed for the use of fluorescence, confocal and atomic force microscopy for the investigation of simulated diving on isolated cells or arteries [14, 15]. Damaged spinal cord tissue due to decompression has been investigated using transmission electron microscopy [16]. Magnetic resonance imaging has been used to detect lesions in bone marrow post-musculoskeletal DCS [17,18]. Additionally, computed tomography (CT) and positron emission tomography (PET) have been investigated for the detection of VGE without indication of sensitivity [19].

Ultrasound Doppler and imaging offer a few noteworthy advantages compared to these imaging modalities. First, ultrasound does not use ionizing radiation inherent to CT and PET, providing a safe way to measure bubbles. Ultrasound monitoring is also capable of real-time measurements, which is not possible with these other modalities. Finally, ultrasound equipment is relatively low-cost and highly portable, allowing for field studies where measurements can be taken directly after a dive (poolside or boat, for example). The relative ease of ultrasound measurements allows for large collections of data that can be acquired at the study site and recorded for (re-)analysis. Nevertheless, ultrasound imaging is more dependent on the operator's acquisition skills and, as will be reviewed subsequently, the physics of bubble behavior under ultrasound need to be carefully considered in interpreting the results.

The role of ultrasound in decompression research

Currently, the primary method to prevent DCS is to perform controlled ascents to allow slow offgassing without significant formation of gas bubbles in tissue. This is achieved by dictating slow ascent rates, with the addition of decompression or safety stops if necessary, where divers pause during their ascent and spend additional time at predetermined depths. The decompression tables and models that dictate these procedures are validated primarily against DCS incidence, aiming to successfully predict DCS risk statistically after a particular dive exposure (profile).

Since DCS is a rare event, studying individual risk factors for the disease is extremely difficult. Therefore, ***statistical models of DCS risk*** for particular profiles or models are used instead, calibrated and validated on a very large number of recorded dive profiles with known outcomes regarding DCS.

In addition, ultrasound (US) monitoring has been used in diving research to detect the VGE formed during decompression. These US-detected VGE are sometimes used as a secondary means of validating statistical models of DCS risk, where dive procedures or profiles that result in higher incidence of VGE being observed post-dive are also discarded. Ultrasound findings have repeatedly shown that VGE are generated routinely in dives and only sometimes result in DCS, while there is additional evidence correlating increasing bubble presence with greater risk for DCS [20-25]. Careful interpretation is required since ultrasound finding do not provide a linear correlation with DCS probability [25]. Moreover, current technologies only allow detection of moving bubbles within the bloodstream.

DCS risk and VGE occurrence are highly variable between individuals as well as within an individual who performs the same dive profiles [26,27]. This variability is currently unexplained with available DCS occurrence data as well as VGE assessment using ultrasound.

Finally, assessment of preconditioning interventions for DCS prevention such as oxygen prebreathing, full-body vibration, antioxidant administration, and exercise regimens have been investigated using bubble and oxidative stress measurements [28].

In diving research, two types of ultrasound monitoring are primarily used: Doppler mode and B-mode echocardiography. These methods can detect VGE that are generated post-decompression. However, the information they provide is different, and each has its own advantages and disadvantages. Before addressing the two modes of ultrasound data acquisition, we review some ultrasound fundamentals in the next section.

Fundamental ultrasound principles

Medical ultrasound monitoring is based on the principle of transmitting high-frequency acoustic pressure waves into the body and detecting reflected (backscattered) echoes from different materials it interacts with. Many of the concepts discussed here are covered in detail in both the Cobbold and Szabo textbooks on ultrasound imaging [29,30].

In short, an ultrasound transducer is used to both generate acoustic waves and detect backscattered signals. Using piezoelectric elements of the transducer (typically ceramics known as lead zirconate titanate or PZT), an electrical signal can be used to generate mechanical energy in the form of pressure waves which are then

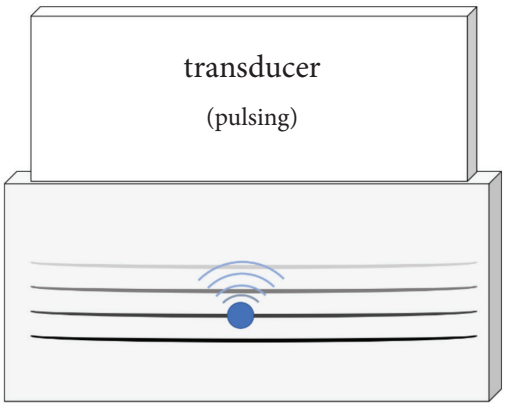

Figure 1: Graphical representation of how propagating waves (black lines) emitted by the transducer are reflected (blue lines) by a scatterer (blue dot) with different acoustic impedance than the surrounding medium back toward the US transducer.

transmitted in the body. The frequency of the wave is known as the number of waves that occur within one second and is measured in terms of Hertz (Hz). Typical ultrasound transducers for medical applications are developed to transmit waves between 1-15 mega-Hertz (MHz). The backscattered echoes from the material being examined (the body) are then converted back into electrical signals which are recorded for generating images or detecting Doppler shifts (explained in more detail in the following section).

Whenever an acoustic wave propagates through a medium and meets another medium with a different acoustic impedance, a portion of the energy continues moving while a portion is reflected (Figure 1). After the wave is generated by the elements of the transducer it passes through matching layers designed to maximize transmission until it reaches the body. Ultrasound coupling gel is used to transmit the wave from the transducer into the tissue, which is mostly water. Larger differences in acoustic impedances result in greater reflected energy back toward the source of the wave. By detecting these pressure waves using an ultrasound transducer, information regarding the position of these materials as well as the motion of an object can be calculated. For example, the acoustic impedance of tissue or blood is approximately 3,000-4,000 times greater than that of an air bubble, resulting in a large reflection that is easily detected by an ultrasound system [31].

The energy generated by the ultrasound transducer is attenuated primarily due to the viscous behavior of the material as well as scattering and diffraction of the wave. Acoustic attenuation is dependent on the material properties but is also a function of frequency and distance. Waves transmitted at a higher frequency lose their energy more quickly than waves at lower frequencies. However, the frequency affects the resolution of the system, with higher frequencies allowing for higher resolution due to a shorter wavelength. As such, a compromise must be made between having higher resolution or greater depth of penetration. This behavior can be seen in Figure 2, where a calibration phantom (tissue mimicking material) is imaged using two different frequencies. In the phantom, scatterers are placed at varying depths in a medium with a constant attenuation.

As acoustic energy is absorbed by the body tissues, two main bioeffects can occur: heating and cavitation. The thermal index (TI) is often displayed on clinical ultrasound imaging scanners and is the ratio between the attenuated power at a region and the estimated power necessary to raise the tissue's temperature by 1 degree C. Often, a device will display thermal indices of soft tissue (TIS), bone (TIB) and cranial bone (TIC). Acoustic cavitation is generation of new bubbles in tissue or the acoustic driving of existing bubbles, with the latter case traditionally separated between inertial and stable cavitation. Stable cavitation is the cyclic oscillation of existing microbubbles, typically induced by low amplitude ultrasound. Inertial cavitation is driven by high-amplitude ultrasound and is characterized by large-magnitude microbubble oscillations that usually result in instability, fragmentation and dissolution of the excited microbubbles. Cavitation can cause mechanical damage to tissues at higher acoustic energies. A measure of how likely acoustic cavitation will occur is the mechanical index (MI), which is the peak negative pressure over the square root of the frequency. In the United States, the Food and Drug Administration requires that ultrasound scanners maintain an MI below 1.9. Both the TI and MI limits have been developed without accounting for bubbles that are formed through decompression. As such, further studies regarding the potential bioeffects of acoustic cavitation of decompression bubbles is warranted, and it is highly suggested that the ALARA principle (as low as reasonably achievable) be applied when using ultrasound to study VGE. The lowest possible MI and TI to achieve a reasonable image/Doppler signal should be used [32].

One last ultrasound physics principle of relevance to decompression bubble detection relates to the unique behavior of bubbles under ultrasound. At low sonication pressures, bubbles can produce non-linear responses if they are insonified near their resonance frequency. This contrasts with tissue that behaves mostly linearly under

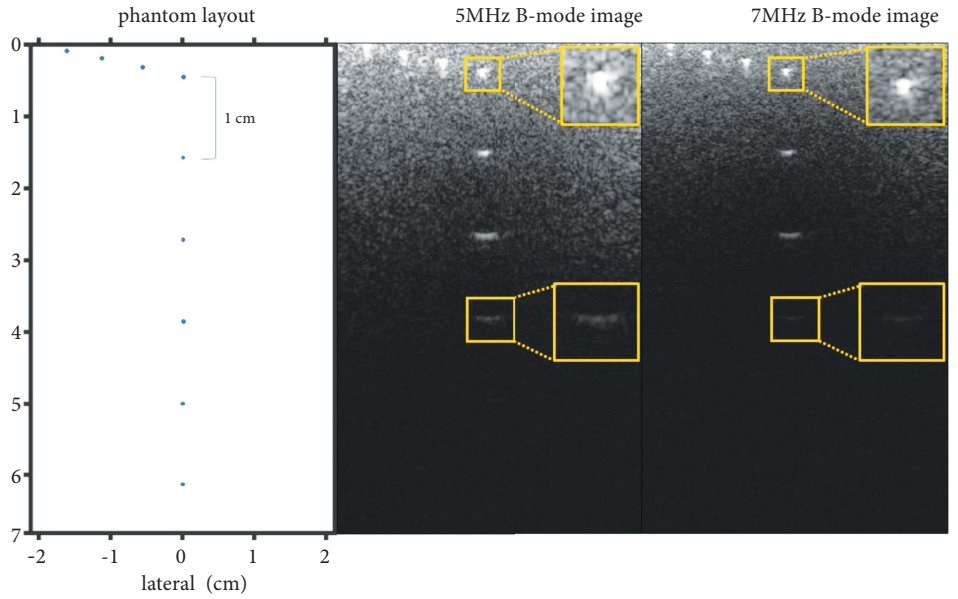

Figure 2: Illustration of frequency-dependent attenuation and resolution tradeoff. The same calibration phantom (with identical scatterers every 1 cm in depth locations, shown in the leftmost panel) can be seen in the two ultrasound images obtained using two different imaging frequencies (5 MHz and 7 MHz) at the same pressure (600 kPa). Scatterers appear sharper in the higher-frequency image. However, due to attenuation, scatterers below 3 cm cannot be detected in the 7-MHz image, unlike the 5-MHz image which is able to detect the 4-cm scatterer.

low-pressure sonication conditions. This principle is used in ultrasound contrast-enhanced vascular imaging, with contrast agents being microbubbles around 1-10 μm in diameter. The implications of this non-linear behavior will be explored thereafter in '*New developments*.' In the meantime, it is worth keeping in mind that for typical frequencies used in cardiac ultrasound imaging (1-4 MHz), the pressure of the signal received is therefore not necessarily a direct measure of the size of the bubble it was reflected from, especially if these bubbles are of the order of a few micrometers. This non-linear behavior complicates direct quantification of microbubble populations.

DOPPLER ULTRASOUND MONITORING

Principle

Doppler ultrasound relies on the detection of the Doppler frequency shift, which is a change in an echo's frequency whenever it reflects off a moving target. Two different tools can be used to measure the Doppler shift: continuous wave (CW) and pulsed wave (PW). The former method employs a continuous wave transmitted from a US transducer and echoes are received at another transducer nearby. In comparison, the pulsed wave scheme uses a single transducer which sends a pulse and listens to the backscattered echoes, allowing for additional information regarding depth. The difference between the transmitted and received frequencies is then used to determine the velocity of the object. Additionally, this frequency difference can be used as an auditory signal due to the shift being within normal hearing range (i.e., 100 Hz–10 kHz) [33]. Whenever a bubble passes through the acoustic field, a chirp-like sound is generated which can be differentiated from blood flow and cardiac function. Therefore, any VGE detectable by Doppler is moving in blood.

Assessment post-dive

The earliest use of diagnostic ultrasound for detecting VGE was in 1968 by Spencer and Campbell [34]. The most common Doppler monitoring site is in the precordium as seen in Figure 3. This location is also considered the gold standard since it allows for sampling of all the blood that passes through the body [35]. Another site used is the subclavian vein, which has been shown to have a stronger association with DCS occurrence [36]. During the examination the subject can be measured during rest or with

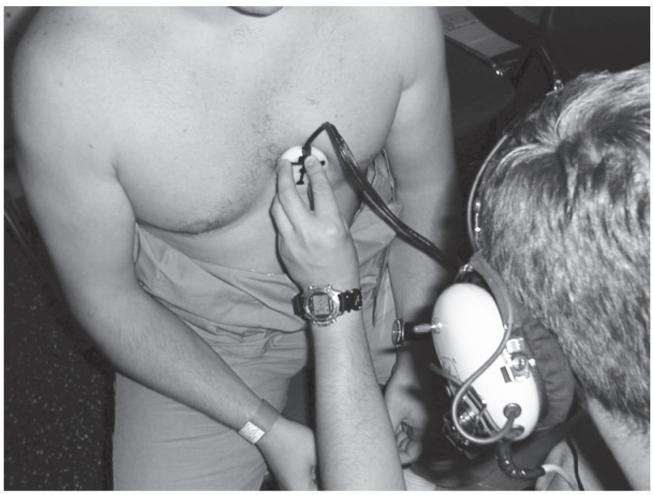

Figure 3: Example of precordial Doppler examination

movement, typically a deep knee bend. These conditions produce different bubble signals, as movement might dislodge bubbles.

In 1974 Spencer and Johanson developed a grading scale for Doppler detection of bubbles using the continuous-wave (CW) Doppler's auditory signal to categorize the degree of bubble movement within a subject [37]. The Spencer code (Table 1) defines five different grades ranging from no bubbles detected to an obscuration of the cardiac signals.

Following the development of the Spencer code, Kisman and Masurel defined their own method for grading bubble signals in Doppler that is more quantitative and allowed for differentiation between various properties of the bubble signals. This Kisman-Masurel (KM) code, shown in Table 2, is separated into three parameter spaces: bubbles per cardiac cycle (frequency); percentage of cardiac cycles with bubbles while at rest or number of cardiac cycles with bubbles after a motion; and amplitude of bubble sounds compared to blood flow and cardiac motion [39]. The KM code can be converted into a Spencer code score; however, the reverse is not possible [38]. Kisman, Masurel and LaGrue further developed a new scoring method that integrates ordinal bubble grades converted from the KM code over four time points, providing an "index of severity" [40]. This index was later renamed to the Kisman Integrated Severity Score (KISS) by Jankowski, et al. [41]. The formula for a KISS score is given in equation 1. The KISS formula was later generalized to be performed with any number of time points instead of just four, as seen in Equation 2. This method of bubble grading allows for comparisons of decompression stress, defined here as Doppler-detectable VGE, using parametric statistics.

An issue that arises with these rating systems is the need for extensive training to produce good inter-rater agreement and reduce variability. In a statistical analysis by Sawatzky and Nishi (1991), a procedure to determine the agreement between raters was developed to determine whether a rater is sufficiently skilled and whether their ratings are reliable, based upon contingency tables and a weighted kappa statistic [42]. The contingency table shows what types of disagreements exist between two raters: scatter, large errors, and bias. Upon determination of the type of disagreement seen, the weighted kappa statistic can be applied, and if a rater achieves a score that shows agreement with well-trained raters, they can also be considered skilled.

Table 1

Grade	Spencer Code
0	Complete lack of bubble signals
1	Occasional bubble signal discernable with the cardiac motion signal, with majority of cardiac periods free of bubbles
2	Many but less than half of the cardiac periods contain bubble signals, singularly or in groups
3	All of the cardiac periods contain showers or single bubble signals, but not dominating or overriding the cardiac motion signals
4	Maximum detectable bubble signal sounding continuously throughout systole and diastole of every cardiac period, and overriding the amplitude of the normal cardiac signals

Spencer code for grading post-dive bubbles (adapted from [38])

Considerations

Doppler ultrasound has found itself to be a mainstay in diving research, primarily due to the low cost and ease of data collection. Most of the research using Doppler uses a continuous-wave Doppler system due to the lower cost of equipment as well as the increased sensitivity to bubble signals since there is no depth compo-

Table2

code	bubbles per cardiac cycle	percentage of cardiac cycles at rest with detectable bubbles	number of cardiac cycles with bubbles after motion	amplitude
0	0	0%	0	no bubbles discernible
1	1-2	1-10%	1-2	barely perceptible
2	several, 3-8	10-50%	3-5	moderate amplitude
3	rolling drumbeat > 9	50-99%	6-10	loud
4	continuous sound	100%	10+	maximal

Kisman-Masurel code for grading post-dive bubbles (adapted from [38])

$$KISS = \frac{100}{4^{\alpha}(t_4 - t_1)} * \frac{[(t_2 - t_1)(d_2^{\alpha} + d_1^{\alpha}) + (t_3 - t_2)(d_3^{\alpha} + d_2^{\alpha}) + (t_4 - t_3)(d_4^{\alpha} + d_3^{\alpha})]}{2} \quad \textbf{(Eq. 1)}$$

$$\underset{KISS}{\text{Generalized}} = \frac{100}{4^{\alpha}(t_n - t_1)} * \sum_{i=1}^{n} \frac{(t_{i+1} - t_i)(d_{i+1}^{\alpha} + d_i^{\alpha})}{2} \quad \textbf{(Eq. 2)}$$

. . . where t is the time of observation in minutes from surfacing, d is the resting precordial Doppler grade 0-4 observed at time t, and α is a constant accounting for the non-linearity of the bubble grading system.

nent. However, pulsed wave has value in providing information where the signal is coming from with the additional depth information. Neither system has a large field of view, where only information directly within the beam-width is obtained.

The aural feedback, however, requires a trained specialist to interpret the corresponding grade for the bubble signal. Both the Spencer and KM grading scales are subjective to the interpreter of the signals; however, the KM code does allow for more reproducible results due to the greater distinction between different components of bubble presence. Furthermore, the KM code allows for means of comparing the agreement of raters to a higher precision than possible with the Spencer code [42].

It should also be noted that a large body of Doppler VGE recordings exists associated with dive profile DCS incidence databases. This data would not be easy to reproduce with other ultrasound technologies due to the large associated time, number of people and costs involved. As such, this data remains useful despite advances in ultrasound technical capabilities due to the possibility of relating it to DCS incidence directly. In this respect, having computer-automated analysis software for this type of recordings, such as proposed by Chappell and Payne to remove user bias, is advantageous [43,44]. Additionally, databases providing Doppler ultrasound of divers are valuable in the development of these automated algorithms, such as the one acquired by Pierleoni, et al. [45].

BRIGHTNESS (B) MODE ULTRASOUND IMAGING

Principle

When ultrasound is pulsed and the backscattered echoes are received at the transducer, a line of electrical data can be recorded as a function of time. The intensities of this line correspond to reflections of the pulsed acoustic wave as it interacts with different materials. The line of voltage versus time is called an amplitude line or A-line. If using a single-element transducer, a B-mode image can be generated by translating the transducer mechanically, accumulating A-lines over a region of interest and performing envelope detection. This method of mechanical steering is one the earliest forms of ultrasound imaging and has since been replaced by multi-element arrays. By applying delays to when elements are transmitting, focusing of the ultrasound wave as well as steering can be achieved over an entire region without translating the transducer. Applying delay-and-sum beamforming to the received signal generates A-lines that can be assembled into a B-mode image.

Interrogated materials that return a greater signal are displayed as bright pixels, whereas low-backscatter media are displayed as dark regions. In the human body, blood has very low echogenicity due to its homogeneity in acoustic impedance, whereas tissue and bone can be seen as brighter regions, as shown in Figure 4.

A benefit of array transducers is the ability to steer beams in directions other than directly in front of the

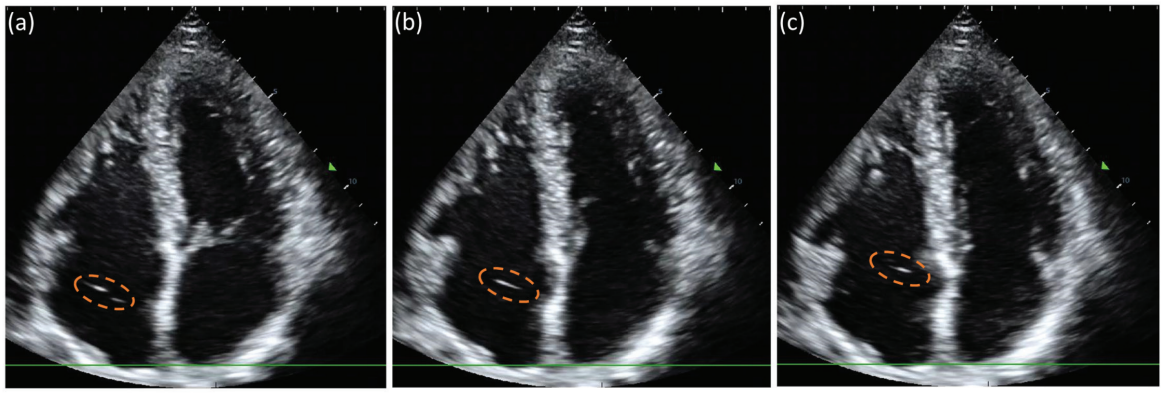

Figure 4: Example echocardiogram of diver showing VGE (circled in orange) in the venous chambers where the valves are open. These are three consecutive frames from the same recording (30 frames per second recording frame rate), showing the two bubbles visible on (a), superimposed in (b), and appearing as a single bright spot in (c) where one might have moved out of plane.

transducer. This is commonly used in phased-array transducers, which have the additional benefit of having a small footprint allowing for imaging between ribs for echocardiography [29,30].

Assessment post-dive

In diving research, it is typical to use B-mode imaging of the heart (echocardiography), where bubbles from the venous system are pumped with blood through the right heart chambers toward the lungs. Due to the echogenicity of bubbles and their motion, they can be identified in the echocardiogram as bright spots inside the dark regions where blood is located.

Echocardiograms can be performed in two ways: through the esophagus (transesophageal or TEE) or through the abdomen/chest (transthoracic or TTE). In TEE, a probe is passed down a person's esophagus and is located near the person's heart. Due to this proximity the image quality is good without much attenuation. However, this procedure carries the potential risk of gastrointestinal tract injury, and sedation is often required, making prolonged and repeated measurements unfeasible [46]. In contrast, TTE is typically performed below or through the ribcage with a phased-array transducer, showing all four chambers of the heart. This method has been seen to be adequate for the detection of VGE due to the high echogenicity of bubbles and is more comfortable for volunteers, allowing for longer studies with more time points in comparison to TEE. Figure 5 shows a TTE echocardiogram being performed on a volunteer.

Figure 5: Example of transthoracic echocardiography examination

TTE is typically performed to show all four chambers of the heart. This is done to evaluate the blood volume inside the right ventricle and atrium where venous blood containing bubbles is moved to the lungs for filtration. If bubbles are visible in the right chambers but not the left, it can be determined that the bubbles are properly filtered by the lungs and no shunting is occurring. Similar to Doppler, measurements at rest and with knee bends are also commonly used with B-mode echocardiography.

Assessment of bubbles in the heart using B-mode echocardiography are evaluated semiquantitatively using the Eftedal and Brubakk (EB) method first developed in 1997. The EB grading scale was developed using six

Table 3

Grade	Eftedal and Brubakk
0	no bubbles
1	occasional bubbles
2	at least one bubble every four cycles
3	at least one bubble per cycle
4	continuous bubbling, at least one bubble per square cm in all frames
5	"white-out," where individual bubbles cannot be discerned

Eftedal and Brubakk scale for grading post-dive echocardiograms (adapted from [38])

grades ranging from no bubbles to white-out, which is when the entire heart is filled with bubbles (Table 3). Eftedal and Brubakk analyzed agreement between raters and demonstrated that untrained raters for images performed as well as partially trained Doppler raters, suggesting greater ease in learning this method [47].

Studies into the interpretability of B-mode echocardiography have shown that increasing grades of bubble presence has a strong correlation with the probability of DCS [25]. The EB grade requires a trained rater and is subject to variability between raters – and within the same rater as well. To account for user bias and reduce analysis time, computer automation of echocardiography VGE analysis was first proposed by Parlak et al. [48,49]. More recently, bubble counting was proposed as a simple method for increasing agreement between untrained raters: The VGE are counted during a frame where the tricuspid valves are open (and less likely to be misidentified as bubbles) for 10 consecutive heart cycles, and the average taken as the bubble count for that recording [50]. The main drawback of this manual counting is that it is time-consuming. However, tools for automating the frame selection and bubble counting are being developed [51–53]. The robustness of any computer-automated VGE detection system ultimately requires a large set of labeled data for training and validation. The main advantage of the bubble-counting method is that it is easy to learn reliably even for previously untrained raters since bubbles are counted only when the tricuspid valves are open, thus avoiding misclassification of valves as VGE. It is therefore possible to distribute this labeling task to many volunteers using this method, and a large collaborative effort to build the necessary database is under way [54].

A newer advancement in cardiac ultrasound imaging is the use of tissue harmonic imaging (THI), which uses higher-pressure waves to generate higher frequency content in the tissue and the bubbles than what was transmitted. Harmonic imaging receives data at these higher harmonic frequencies (multiples of the transmitted frequency) and suppresses the original transmitted frequency signal. Since the acoustic signal used to generate an image is generated within the medium there is a reduction in reverberation artifacts, and the higher pressure is typically useful for subjects with excess adipose tissue. The higher-frequency data generates a higher-resolution image, resulting in increasing adoption of this imaging mode. To date the only comparison between THI and conventional B-mode imaging for assessing VGE did not show any statistically significant differences in EB grades [55].

Considerations

Like Doppler, B-mode ultrasound is not immune to variability with regard to decompression bubble quantification. Many devices are available on the market for researchers to purchase, each with their own proprietary implementations of image acquisition and processing. Additionally, the transducer that is used will affect the range of frequencies available and the field of view for the image produced. The image quality is affected by the frequency used. Lower frequencies allow for deeper penetration, making it easier to image the heart, but the resolution is decreased, impeding the ability to differentiate between bubbles. In diving research, phased-array transducers with a frequency range of 1-4 MHz are typically used for transthoracic echocardiography.

Ultrasound machines have the ability to apply time gain compensation (TGC), which increases the pixel intensity depending on the depth within the image. The purpose for this feature is to counteract reduced intensities due to the attenuation of the ultrasound pressure as it passes through tissue. In general, sonographers change this value so that the image is uniform in brightness over depth. However, if quantitative assessment of bubble brightness is desired (for bubble sizing), the TGC will affect the results. Additionally, if bubble signal is weak, increasing the gain will improve the signal, but electrical noise will be increased, concurrently resulting in a "snow-like" appearance in dark regions. Thus, it is generally recommended that TGC and gain be used to produce a high-quality image where the tissue of the heart can be seen with even brightness through depth without

increasing noise substantially. Finally, many ultrasound manufacturers provide speckle removal or additional proprietary (black-box) visual enhancement of cardiac tissue structures that have been developed without VGE applications in mind, which may artificially suppress those signals.

It is typically difficult to acquire echocardiograms due to the necessity of imaging between the ribs. Also, with patient movement, primarily from respiration, the heart can move out of the imaging plane. Grading of echocardiograms can be easier than using the Spencer or KM codes with Doppler since it is in a visual medium and the grading scale is straightforward. Bubble-counting methods that try to further quantify bubble appearance can be slow and tedious without any automation processes.

Furthermore, the importance of the measurement protocol with respect to diving time has been established [43,55]. The amount of bubbles quantified indeed varies over time after the diver surfaces, and precisely timing the measurements is therefore important for comparing different procedures or investigating inter- or intrapersonal differences in VGE. This variability has been demonstrated with Doppler aural recordings [56], as well as B-mode echocardiography analyzed through both grading [57] and bubble-counting [26]. The time course for VGE growth and circulation is dynamic and as such, comparisons between different studies should account for this behavior [26].

PRACTICAL CONSIDERATIONS AND NEW DEVELOPMENTS

Even though Doppler ultrasound and B-mode echocardiography are still in wide use today, there are some limitations and challenges with these methods that need to be addressed. Some of the major issues are: 1) dependence on the operator collecting the data; 2) data interpretation is rater-dependent and time-consuming; 3) time-series monitoring is inadequately sampled temporally; and 4) these methods are only assessing moving bubbles in blood and not useful for determining their size. All of these points could influence physiological interpretations.

Practical considerations

Although ultrasound is often used in diving research, standardization is key to well-designed studies that allow comparisons between different research groups. We refer the reader to the consensus guidelines developed in 2016 which detail practical considerations for decompression study design using ultrasound imaging and remain the current best practice [58]. The consensus guidelines for the use of ultrasound for diving research was developed in 2016 at the International Meeting on Ultrasound for Diving Research and produced a standardized method to design research protocols. In short, these guidelines discuss 1) data acquisition methods, 2) methods to grade the ultrasound data, 3) considerations for data interpretation, and 4) best practices for maintaining/reporting data. Without reproducing all details, some recommendations from the guideline that should be emphasized are that measurements should be conducted for at least 120 minutes from the completion of the decompression period and recorded at intervals of 20 minutes or less [58]. This measurement schedule is required to adequately sample the variable VGE formation and circulation over time, which has been observed previously [26,56,57]. As previously discussed, imaging settings may influence bubble quantification; thus recording and reporting these can be useful for data interpretation. For this, we recommend including the ultrasound machine model, probe model, acquisition mode used (e.g., "adult cardiac") and settings (at a minimum the operating frequency and MI). Of note is that some systems have proprietary optional packages that can despeckle/smooth cardiac images. We do not recommend using these, as they are not developed with VGE detection in mind and may influence VGE quantification. We have also found it useful to perform a preliminary VGE assessment at the point of acquisition because ultrasound images are easier to interpret while probe placement is known and can be adjusted in real time to ensure best image quality. For this, the operator records their preliminary assessment as either binary bubble presence, or preliminary grade assessment for experienced operators.

Hardware and software advancements

Since the early 2010s there have been technological leaps in both the system hardware and image processing for ultrasound imaging. Portable devices such as the FujiFilm Sonosite iViz (Bothell, Washington) and the GE Vscan (GE Healthcare, Chicago, Illinois) are all-in-one systems that have both the ultrasound display and transducers in one package. Additionally, new advances in mobile phone technology has led to the Philips Lumify (Andover, Massachusetts) and Butterfly IQ (Guilford, Connecticut), which are transducers directly attached

to a smartphone for image processing and display. The Butterfly IQ has also implemented feedback systems that aid in the acquisition of improved quality data without extensive sonography experience. The Butterfly IQ also uses capacitive micromachined ultrasound transducers (CMUT) in place of piezoelectric crystal-based elements [59]. This newer transducer technology has the advantage of supporting a larger range of available frequencies (bandwidth). In the case of the Butterfly IQ this allows for a single probe to perform as a linear, curved and phased-array transducer with different frequencies for different imaging applications, including TTE with customizable beam steering [60]. Although VGE have been detected post dive using the Butterfly IQ (personal author experience), VGE quantification using this system has yet to be formally evaluated. The increased portability of these new devices may make them more attractive to researchers as well as divers. Development of products such as the O-dive (Azoth Systems, Ollioules, France), which is a subclavian Doppler VGE device advising on dive profile modifications, shows that there is increasing interest from the dive community to personalize their own decompression.

Additionally, new transducers are being developed to allow for dual-frequency imaging where a region can be insonified at a lower pressure (1-3 MHz) and high-frequency content can be recorded if superharmonics are generated (15-30 MHz) that can be observed in lipid-shelled microbubbles used in clinical diagnostic ultrasound imaging [61].

Finally, a limitation with conventional two-dimensional imaging using one-dimensional arrays is that information is obtained only within the imaging plane, which is the physical volume that the transducer can image at one moment. However, decompression bubbles are non-static and move throughout a larger region than is normally scanned. As such, advances in three-dimensional imaging are being made whereby the mechanical scanning of a 1-D array or the use of a 2-D array allows for volumetric imaging in real time. This technology would allow for improved quantification of VGE but will increase the need for automated methods of analysis.

Bubble sizing

In diagnostic ultrasound imaging, contrast agents consisting of encapsulated microbubbles are used to enhance the contrast from within the vasculature, a technique known as contrast-enhanced ultrasound (CEUS). Due to the large difference in acoustic impedance between the gas in the bubbles and the surrounding medium, there is a large reflection of the ultrasound back to the transducer. Additionally, a bubble will oscillate when insonified, where at positive pressures the bubble will compress and negative pressures result in expansion. Uneven expansion and contractions of the bubble generates non-linear pressure waves from the bubbles [62,63]. This non-linearity is not exhibited in tissue at low mechanical indices less than 0.4 and can therefore be leveraged to differentiate between bubbles and tissue. Additionally, microbubble resonance is highly dependent on its size. A bubble with a specific radius will have a related "resonant frequency," which is the frequency at which the bubble generates the greatest acoustic signal (maximal radius change under oscillations). However, the frequency range of clinical transducers which could potentially be used to detect microbubble harmonic content corresponds only to bubbles less than 5 μm in diameter [64]. Nevertheless, it is not possible to directly relate microbubble contrast agent behavior to VGE due to the lack of information on VGE size and composition.

Buckey, et al. (2005) developed a dual-frequency system that allowed for the sizing of bubbles by finding the frequency at which the bubbles return the greatest signal. Bubbles are "pumped" or insonified continuously using a lower frequency that allows them to resonate, and a secondary pulse of a higher frequency is used to image the volume. This is achieved by aligning multiple transducers to a same small volume, so this technique interrogated a "point" (small volume) where the setup is positioned. Bubbles that are interrogated at their resonant frequency by the pump signal will return a signal that has non-linear mixing of the low- and high-frequency waveforms, meaning that the sum and difference of these two signals will be presented in the frequency domain. By using the Fourier transform, the frequency components of the signal can be extracted, and the magnitude of theses sideband signals represents the relationship between the pump frequency and the bubble resonant frequency. Through finding the pump frequency at which this magnitude is maximized, the bubble radius can be determined [65]. This dual-frequency approach has been demonstrated to be sensitive to microbubbles below the theoretical limit of detection of B-mode and Doppler ultrasound. In particular, Swan, et al. have shown that microbubbles in tissues are detectable post-decompression in swine [66], and other work has shown that microbubbles may be generated in

the body even without changes in ambient pressure [67].

In addition to probing one small tissue region it is also possible to leverage this microbubble non-linear behavior to create images within tissues where microbubble signals are localized in the plane of view of the transducer. Due to the harmonic signal generated by microbubbles it is possible to use techniques similar to tissue harmonic imaging to quantify bubbles smaller than VGE in the 1- to 10-μm diameter range. In tissue harmonic imaging, non-linear signals are generated by using a high pressure to allow for the deformation of the propagating wave in tissue. In microbubble-specific harmonic imaging, low pressures are maintained to prevent tissue harmonics while microbubbles are still able to produce non-linear signals. A common approach is to use multi-pulse schemes such as pulse inversion, amplitude modulation, or a combination of the two. We have recently demonstrated that this method allows for larger bubbles to be suppressed within the ultrasound image due to their linear resonant behavior, leaving mostly microbubble signals in the final image [68]. A comparison of the performance of different multi-pulse schemes for this application is also under way in our laboratory [69]. In a preliminary proof-of-principle experiment imaging seven divers with a commercially available cardiac contrast-enhanced imaging mode, microbubbles were detected post-dive even when no VGE were quantified on B-mode, in both venous and arterial circulation, and these followed a different time course than VGE [70]. We have also demonstrated that ultra-high frame rates are necessary for optimizing microbubble quantification with this technique since large bubble cancellation is affected by bubble movement [71]. This can be mitigated by the recent development of plane-wave cardiac CEUS at more than 5,000 frames per second (fps), recently shown feasible as an imaging method in humans for the first time [72]. Instead of requiring multiple ultrasound transmissions to generate lines for an image, a single plane-wave transmission can be used to generate an image, increasing the possible frame rate from ~30 fps in conventional scanners up to 10,000 fps depending on the desired imaging depth.

These new imaging techniques open the door to investigating microbubble VGE precursors and potentially provide a better understanding of decompression bubble formation. They could also be used to directly assess preconditioning effects on pre-existing microbubble populations. An important consideration with all non-linear methods for bubble detection is the fact that they do not depend on bubble motion, and as such decompression bubbles of resonant size can theoretically be detected. These techniques may provide the ability to detect and visualize stationary bubbles in tissue.

CONCLUSIONS

Ultrasound monitoring has been used for dive research since the late 1960s. Due to the highly echogenic nature of bubbles they are easily detected in the circulation by using either Doppler or B-mode imaging. Both methods have been well developed and provide semiquantitative measures of bubble presence. However, there are still issues that need to be addressed, such as the lingering variability between raters and the discontinuous data-gathering. Quantitative and continuous measurements of bubbles are the next step in the development of ultrasound technologies for the study of decompression. As new ultrasound devices are developed we should expect to see an even wider use of ultrasound in diving research as well as means to investigate bubbles in new ways. ■

Acknowledgments

V.P. gratefully acknowledges funding from the Divers Alert Network as DAN Scholar. This review is related to activities funded through the Divers Alert Network (grant #DAN-UNC-1, and previously DAN/R.W. (Bill) Hamilton Memorial Dive Medicine Research Grant administered by the Women Divers Hall of Fame).

REFERENCES

1. Vann RD, Butler FK, Mitchell SJ, Moon RE. Decompression illness. Lancet. 2011;377(9760):153-164.

2. Webb JT, Olson RM, Krutz RWJ, Dixon G, Barnicott PT. Human tolerance to 100% oxygen at 9.5 psia during five daily simulated 8-hour EVA exposures. Aviat Space Environ Med. 1989 May;60(5):415-421.

3. Kindwall EP. Compressed air tunneling and caisson work decompression procedures: development, problems, and solutions. Undersea Hyperb Med. 1997;24(4):337-345.

4. Boyle R. New pneumatical experiments about respiration. Philos Trans R Soc London. 1670 Jan;5(62):2011-2031.

5. Bert P. La pression barométrique. Recherches de physiologie expérimentale. G. Masson; 1878.

6. Hill L, Macleod JJR. Caisson illness and diver's palsy. An experimental study. J Hyg (Lond). 1903;3(4):401-445.

7. Calder IM. Dysbarism. A review. Forensic Sci Int. 1986 Apr;30(4):237-266.

8. Papadopoulou V, Eckersley RJ, Balestra C, Karapantsios TD, Tang M-X. A critical review of physiological bubble formation in hyperbaric decompression. Adv Colloid Interface Sci. 2013 May;191-192:22-30.

9. Papadopoulou V, Tang M-X, Balestra C, Eckersley RJ, Karapantsios TD. Circulatory bubble dynamics: From physical to biological aspects. Adv Colloid Interface Sci. 2014 Apr;206: 239-249.

10. Walsh C, Stride E, Cheema U, Ovenden N. A combined three-dimensional in vitro-in silico approach to modelling bubble dynamics in decompression sickness. J R Soc Interface. 2017 Dec 31;14(137).

11. Papadopoulou V, Evgenidis S, Eckersley RJ, et al. Decompression induced bubble dynamics on ex vivo fat and muscle tissue surfaces with a new experimental set up. Colloids Surfaces B Biointerfaces. 2015;129:121-129.

12. Gersh I, Catchpole HR. Appearance and distribution of gas bubbles in rabbits decompressed to altitude. J Cell Comp Physiol. 1946 Dec;28(3):253-269.

13. Gersh I, Hawkinson GE, Jenney EH. Comparison of vascular and extravascular bubbles following decompression from high pressure atmospheres of oxygen, helium-oxygen, argon-oxygen and air. J Cell Comp Physiol. 1945 Oct;26(2):63-74.

14. Wang Q, Belhomme M, Guerrero FF, Mazur A, Lambrechts K, Theron M. Diving under a microscope - A new simple and versatile in vitro diving device for fluorescence and confocal microscopy allowing the controls of hydrostatic pressure, gas pressures, and kinetics of gas saturation. Microsc Microanal. 2013;19(3):608-616.

15. D'Agostino DP, Mcnally HA, Dean J, Technology CE, Lafayette W. Development and testing of hyperbaric atomic force microscopy (AFM) and fluorescence microscopy for biological applications. J Microsc. 2012 May;246(2):129-142.

16. Francis TJR, Pezeshkpour GH, Dutka AJ, Hallenbeck JM, Flynn ET. Is there a role for the autochthonous bubble in the pathogenesis of spinal cord decompression sickness? J Neuropathol Exp Neurol. 1988 Jul;47(4):475-487.

17. Stéphant E, Gempp E, Blatteau J-E. Role of MRI in the detection of marrow bubbles after musculoskeletal decompression sickness predictive of subsequent dysbaric osteonecrosis. Clin Radiol. 2008 Dec;63(12):1380-1383.

18. Gempp E, Louge P, Lafolie T, Demaistre S, Hugon M, Blatteau JE. Relation between cervical and thoracic spinal canal stenosis and the development of spinal cord decompression sickness in recreational scuba divers. Spinal Cord. 2014 Mar 15; 52(3):236-240.

19. Hansen K, Schmidt N, Pedersen M. CT, PET and MRI in experimental barometric physiology. FASEB J. 2015 Apr 1;29 (S1):678.15.

20. Pontier J-M, Guerrero F, Castagna O. Bubble formation and endothelial function before and after 3 months of dive training. Aviat Space Environ Med. 2009 Jan;80(1):15-19.

21. Lubbers J, van den Berg JW. An ultrasonic detector for microgasemboli in a bloodflow line. Ultrasound Med Biol. 1977;2(4):301-310.

22. Van Liew HD, Conkin J, Burkard ME. How big are decompression-sickness bubbles. In: Proceedings of the XIXth Annual Meeting of European Undersea Biomedical Society Trondheim, Norway: SINTEF Unimed. 1993. p. 258-262.

23. Hills BA, Butler BD. Size distribution of intravascular air emboli produced by decompression. Undersea Biomed Res. 1981 Sep;8(3):163-170.

24. Lee J, Kentish S, Ashokkumar M. Effect of surfactants on the rate of growth of an air bubble by rectified diffusion. J Phys Chem B. 2005 Aug;109(30):14595-14598.

25. Doolette DJ. Venous gas emboli detected by two-dimensional echocardiography are an imperfect surrogate endpoint for decompression sickness. Diving Hyperb Med. 2016 Mar;46(1): 4-10.

26. Papadopoulou V, Germonpré P, Cosgrove D, et al. Variability in circulating gas emboli after a same scuba diving exposure. Eur J Appl Physiol. 2018 Jun 3;118(6):1255-1264.

27. Papadopoulou V, Tillmans F, Denoble P. Call for a multicenter study on the intra-subject variability of venous gas emboli. Undersea Hyperb Med. 2017;44(5):377.

28. Germonpre P, Balestra C. Preconditioning to reduce decompression stress in scuba divers. Aerosp Med Hum Perform. 2017 Feb;88(2):114-120.

29. Cobbold RSC. Foundations of biomedical ultrasound. Oxford University Press; 2006.

30. Szabo TL. Diagnostic ultrasound imaging: inside out. Academic Press; 2004.

31. Nishi RY. The scattering and absorption of sound waves by a gas bubble in a viscous liquid. Acta Acust united with Acust. 1975;33(2):65-74.

32. Abbott JG. Rationale and derivation of MI and TI - A review. Ultrasound Med Biol. 1999;25(3):431-441.

33. Evans DH, McDicken WN. Doppler ultrasound: physics, instrumentation and signal processing. John Wiley & Sons; 2000.

34. Spencer MP, Campbell SD. Development of bubbles in venous and arterial blood during hyperbaric decompression. Bull Mason Clin. 1968;22:26-32.

35. Pollock NW. Use of ultrasound in decompression research. Diving Hyperb Med. 2007;37(2):68-72.

36. Hugon J, Metelkina A, Barbaud A, et al. Reliability of venous gas embolism detection in the subclavian area for decompression stress assessment following scuba diving. Diving Hyperb Med J. 2018 Sep 30;48(3):132-140.

37. Spencer MP, Johanson DC. Investigation of new principles for human decompression schedules using Doppler ultrasonic blood bubble detection. Institute of Environmental Medicine and Physiology, Seattle, WA; 1974.

38. Brubakk AO, Neuman TS. Bennett and Elliott's Physiology and Medicine of Diving. Saunders Book Company; 2003. 501-529.

39. Kisman KE, Masurel G, Guillerm R. Bubble evaluation code for Doppler ultrasonic decompression data. Undersea Biomed Res. 1978;5:28.

40. Kisman K, Masurel G, Lagrue D, Le Pechon JC. Evaluation de la qualité d'une décompression basée sur la détection ultrasonore de bulles. Med Aeronaut Spat - Med Subaquat Hyperb. 1978;17(67):293-297.

41. Jankowski LW, Nishi RY, Eaton DJ, Griffin AP. Exercise during decompression reduces the amount of venous gas emboli. Undersea Hyperb Med J Undersea Hyperb Med Soc Inc. 1997;24(2):59-65.

42. Sawatzky KD, Nishi RY. Assessment of inter-rater agreement on the grading of intravascular bubble signals. Undersea Biomed Res. 1991;18(5-6):373-396.

43. Payne SJ, Chappell MA. Automated determination of bubble grades from Doppler ultrasound recordings. Aviat Space Environ Med. 2005 Aug;76(8):771-777.

44. Chappell MA, Payne SJ. A method for the automated detection of venous gas bubbles in humans using empirical mode decomposition. Ann Biomed Eng. 2005;33(10):1411-1421.

45. Pierleoni P, Mercuri M, Belli A, Pieri M, Marroni A, Palma L. Doppler ultrasound dataset for the development of automatic emboli detection algorithms. Data Br. 2019;27:104739.

46. Côté G, Denault A. Transesophageal echocardiography-related complications. Can J Anesth Can d'anesthésie. 2008 Sep; 55(9):622-647.

47. Eftedal O, Brubakk AO. Agreement between trained and untrained observers in grading intravascular bubble signals in ultrasonic images. Undersea Hyperb Med. 1997;24(4):293-299.

48. Parlak IB, Egi SM, Ademoglu A, et al. A neuro-fuzzy approach of bubble recognition in cardiac video processing. In: International Conference on Digital Information and Communication Technology and Its Applications. Springer; 2011.. 277-286.

49. Parlak BI, Egi SM, Ademoglu A, et al. Intelligent bubble recognition on cardiac videos using Gabor wavelet. Int J Digit Inf Wirel Commun. 2011;1(3):229-237.

50. Germonpré P, Papadopoulou V, Hemelryck W, et al. The use of portable 2D echocardiography and "frame-based" bubble counting as a tool to evaluate diving decompression stress. Diving Hyperb Med. 2014 Mar;44(1):5-13.

51. Papadopoulou V, Hui J, Balestra C, et al. Automated counting of venous gas emboli in post-scuba dive echocardiography. In: The Proceedings of IEEE International Ultrasonics Symposium, (IUS). 2013 July 21-25; Prague, Czech Republic; 2013.

52. Markley E, Le DQ, Germonpré P, et al. A fully automated method for late ventricular diastole frame selection in post-dive echocardiography without ECG gating. In: The Proceedings of the 2019 European Underwater and Baromedical Society (EUBS) conference. 2019 September 9-12; Tel Aviv, Israel; 2019.

53. Le DQ, Kierski T, Markley E, et al. A deep-learning approach for automated bubble counting in 2D echocardiography of divers. In: The Proceedings of the Undersea and Hyperbaric Medicine Society (UHMS) Annual Scientific Meeting. 2019 June 27-29; Rio Mar, Puerto Rico, USA; 2019.

54. Barrentine B, Le DQ, Germonpré P, et al. A graphical user interface for expediting bubble-counting analysis of post-dive echocardiograms and statistics for vetting crowdsourcing contributions. In: The Proceedings of the Undersea and Hyperbaric Medicine Society (UHMS) Annual Scientific Meeting. 2019 June 27-29; Rio Mar, Puerto Rico, USA; 2019.

55. Blogg SL, Gennser M, Møllerløkken A, Brubakk AO. Ultrasound detection of vascular decompression bubbles: the influence of new technology and considerations on bubble load. Diving Hyperb Med. 2014 Mar;44(1):35-44.

56. Cialoni D, Pieri M, Balestra C, Marroni A. Dive risk factors, gas bubble formation, and decompression illness in recreational SCUBA diving: analysis of DAN Europe DSL data base. Front Psychol. 2017 Sep 19;8:1587.

57. Ljubkovic M, Zanchi J, Breskovic T, Marinovic J, Lojpur M, Dujic Z. Determinants of arterial gas embolism after scuba diving. J Appl Physiol. 2011;112(1):91-95.

58. Møllerløkken A, Blogg SL, Doolette DJ, Nishi RY, Pollock NW. Consensus guidelines for the use of ultrasound for diving research. Diving Hyperb Med. 2016 Mar;46(1):26-32.

59. Joyce YLB, Jiajun XM, Flemming FP, Ji-Bin LMF. CMUT/CMOS-based Butterfly iQ - A Portable Personal Sonoscope. Adv Ultrasound Diagnosis Ther. 2019;3(3):115.

60. Clevert DA, Schwarze V, Nyhsen C, D'Onofrio M, Sidhu P, Brady AP. ESR statement on portable ultrasound devices. Insights Imaging. 2019;10(1).

61. Gessner RC, Frederick CB, Foster FS, Dayton PA. Acoustic angiography: a new imaging modality for assessing microvasculature architecture. J Biomed Imaging. 2013;2013:14.

62. Goertz DE, Needles A, Burns PN, Foster FS. High-frequency, nonlinear flow imaging of microbubble contrast agents. IEEE Trans Ultrason Ferroelectr Freq Control. 2005;52(3):495-502.

63. Leighton TG. The forced bubble. In: The Acoustic Bubble. Elsevier; 1994. 287-438.

64. de Jong N, Bouakaz A, Frinking P. Basic acoustic properties of microbubbles. Echocardiography. 2002 Apr;19(3):229-240.

65. Buckey JC, Knaus DA, Alvarenga DL, Kenton MA, Magari PJ. Dual-frequency ultrasound for detecting and sizing bubbles. Acta Astronaut. 2005;56(9-12):1041-1047.

66. Swan JG, Bollinger BD, Donoghue TG, et al. Microbubble detection following hyperbaric chamber dives using dual-frequency ultrasound. J Appl Physiol. 2011;111(5):1323-1328.

67. Wilbur JC, Phillips SD, Donoghue TG, et al. Signals consistent with microbubbles detected in legs of normal human subjects after exercise. J Appl Physiol. 2009;108(2):240-244.

68. Hensel JSE, Le DQ, Balestra C, Tang M-X, Dayton PA, Papadopoulou V. Adapting contrast-enhanced imaging techniques to improve quantification of decompression bubbles in humans. In: The Proceedings of the Undersea and Hyperbaric Medicine Society (UHMS) Annual Scientific Meeting. 2018 June 28-30; Lake Buena Vista, Florida, USA; 2018.

69. Le DQ, Palakurthi M, Evgenidis S, et al. Comparison of non-linear ultrasound imaging strategies for the detection of decompression microbubbles. In: The Proceedings of the 2019 European Underwater and Baromedical Society (EUBS) conference. 2019 September 9-12; Tel Aviv, Israel; 2019.

70. Papadopoulou V, Balestra C, Theunissen S, et al. Can current contrast mode echocardiography help estimate bubble population dynamics post-dive? In: The Proceedings of the 2017 European Underwater and Baromedical Society (EUBS) conference. 2017 September 13-16; Ravenna, Italy; 2017.

71. Hensel JSE, Le DQ, Balestra C, Tang M-X, Dayton PA, Papadopoulou V. Nonlinear microbubble ultrasound imaging for improved decompression stress quantification in humans. In: The Proceedings of the 23rd European symposium on Ultrasound Contrast Imaging. 2018 January 18-19; Rotterdam, Netherlands; 2018.

72. Toulemonde MEG, Corbett R, Papadopoulou V, et al. High frame-rate contrast echocardiography: In-human demonstration. JACC Cardiovasc Imaging. 2018;11(6):923-924.

✦